Journal of Applied Polymer Science

Synergistic effect of expandable graphite and aluminum hypophosphite on flame-retardant properties of rigid polyurethane foam

Wen-Zong Xu,[1,2] Liang Liu,[1] Shao-Qing Wang,[1] Yuan Hu[2]

[1]Department of Polymer Materials, School of Materials Science and Chemical Engineering, Anhui Jianzhu University, Hefei, Anhui Province 230601, People's Republic of China

[2]State Key Lab of Fire Science, University of Science and Technology of China, Hefei, Anhui 230026, People's Republic of China

Correspondence to: W. Z. Xu (E-mail: wenzongxu@ahjzu.edu.cn)

ABSTRACT: A series of flame retarding rigid polyurethane foam (RPUF) composites based on expandable graphite (EG) and aluminum hypophosphite (AHP) were prepared by the one-pot method. The properties were characterized by limiting oxygen index (LOI) test, cone calorimeter test, thermogravimetric analysis (TGA), real-time Fourier transform-infrared spectra (RT-FT-IR), X-ray photoelectron spectroscopy (XPS), scanning electron microscopy (SEM), etc. The results indicate that both EG and AHP could enhance the flame retardency of RPUF composites. Besides, the flame retardant effect of EG was better than that of AHP. The results also show that partial substitution of EG with AHP could improve the flame retardency of RPUF, and EG and AHP presented an excellent synergistic effect on flame retardancy. What is more, compared with RPUF/20EG and RPUF/20AHP, the heat release rate (HRR) and total heat release (THR) of RPUF/15EG/5AHP were lower.TGA results indicate that partial substitution of EG with AHP could improve the char residue which provided better flame retardancy for RPUF composites. The thermal degradation process of RPUF composites and the chemical component of the char residue were investigated by RT-FT-IR and XPS. And the results prove that RPUF/15EG/5AHP had higher heat resistance in the later stage. Compared with the RPUF composites filled with EG, a better cell structure and mechanical properties were observed with the substitution of AHP for part of EG. © 2015 Wiley Periodicals, Inc. J. Appl. Polym. Sci. **2015**, *132*, 42842.

KEYWORDS: composites; flame; foams; polyurethanes; retardance

Received 2 May 2015; accepted 14 August 2015

DOI: 10.1002/app.42842

INTRODUCTION

Rigid polyurethane foam (RPUF) is a kind of structure and thermal insulation material, which can withstand a certain load without obvious deformation. It is extensively used in various fields,[1–3] such as construction, transportation, petrochemical engineering, aeronautics, and astronautics due to its low density, high compressive strength, superior dimensional stability, lower thermal conductivity, and good cohesiveness.[4–7] However, pure RPUF is flammable because it consists of a large number of aliphatic segments and possesses a porous cellular structure.[3] When RPUF is exposed to heat, it burns rapidly with the release of smoke containing CO, HCN, and other toxic gases which are very harmful to the health and environment and restricts its application in various fields.[8] Therefore, more and more efforts have been made to improve the flame retardancy of RPUF.

In recent years, the simplest way to prevent the burning of RPUF is to add flame retardant additives.[9] The commonly used additives are halogen, phosphorus, nitrogen flame retardants, such as decabromodiphenyl ethane (DBDPE),[10] dimethyl methylphosphonate (DMMP),[11] ammonium polyphosphate (APP),[12] and melamine cyanurate.[13] Expandable graphite (EG) is a novel intumescent flame retardant, and it not only endows polymer materials with good flame retardancy but is also low-cost and environmentally friendly. EG is a special type of graphite flake which can expand immediately and generate a voluminous insulative char layer covering the surface of a polymer matrix at high temperature. The char layer acts as a physical barrier to limit the diffusion of combustible volatile products towards the flame zone while inhibiting oxygen or heat towards the polymer to prevent the burning of the underlying polymer material.[14] Shi *et al.*[15] studied the effect of different-sized expandable graphite particles on the flame retardancy of high-density RPUF. Their results showed that RPUF filled with larger particle size EG exhibits better flame retardant properties than RPUF filled with smaller particle size EG. Meng *et al.*[16] and Thirumal *et al.*[17] also discussed the effect of EG on the flame retardant properties of RPUF and concluded that increasing the EG

content significantly improves the flame retardancy of materials. However, the char layer of EG after burning is noncompact and the EG particles would deteriorate the mechanical properties of RPUF, which limits its fire retardant applications.

Aluminum hypophosphite (AHP) is a non-toxic, non-migration and environmentally friendly flame retardant.[18] Hence, AHP has considerable applications in many polymer materials as an excellent halogen-free flame retardant, with a pretty good effect.[19–22] AHP has also been reported as an effective flame retardant for RPUF. Lorenzetti *et al.*[23] found that AHP could enhance the flame retardancy of RPUF. When the content of AHP was 10 wt %, the LOI value of RPUF composites increased to 26.5 vol % from 20.1 vol % of pure RPUF, and the heat release rate also decreased. But the flame retardant efficiency of AHP is limited.

So far, a few studies have been focused on the flame retardancy of RPUF filled with EG and AHP.[24] In this work, EG and AHP were added into the RPUF system with different ratios by cast molding. The flame retardant and thermal properties of RPUF composites were evaluated by LOI test, cone calorimeter test, and TGA. The thermal degradation process of RPUF composites was investigated by RT-FT-IR and the chemical components of the char residue were explored by XPS. In addition, the synergistic flame retardant effects with EG and AHP in RPUF composites were also investigated.

EXPERIMENTAL

Materials

EG (average particle size: 270 μm; expansion rate: 50 mL/g; set-off temperature: 220°C) was purchased from the Shijiazhuang ADT Carbonic Material Factory, China. AHP (average particle size: 10 μm) was purchased from Qingzhou Yichao Chemical Co., Ltd., China. Polyether polyol (viscosity at 25°C: 3283 mPas; typical hydroxyl value: 430 mg KOH/g; functionality: 4.1; average molecular weight: 550 g/mol) was purchased from Gaoqiao Petro Co., Ltd., China. Polyaryl polymethylene isocyanate (PAPI) (-NCO weight percent: 31 wt %; viscosity at 25°C: 150–250 mPas) was purchased from German Basf (China) Co., Ltd. Triethylenediamine (A-33; a dipropylene glycol solution of triethylenediamine; mass fraction of 33%) was purchased from Air Products and Chemicals, Inc. Dibutyl tin dilaurate(T_{12}) was purchased from Sinopharm Chemical Reagent Co., Ltd., China. 1,1-Dichloro-1-fluoroethane (HCFC-141b) was purchased from German Basf (China) Co., Ltd. Distilled water was made in our laboratory. Silicone oil was purchased from Qindao Zhongbao Chemical Co., Ltd., China.

Foam Preparation

Pure RPUF samples were prepared by the conventional one-pot method. Chemical compositions of the pure RPUF are shown in Table I. All components except PAPI were mixed and stirred with an electric stirrer until a uniform mixture was obtained at room temperature. PAPI was then added quickly into the mixture and was stirred for an additional 20 s. Then, the mixture was poured immediately into the cast mold completely covered with a lid. When frothy bubbles formed, the mold was placed into an oven and heated at 100°C for 4 h to accelerate the curing process. Finally, the foam was removed from the mold. RPUF filled with EG and AHP were prepared similarly, and they were mixed with other components before adding PAPI. The contents of EG or AHP ranged from 0 to 20 wt %. All samples were cut into the desired shapes and sizes according to the corresponding testing standards for the evaluation of different properties.

Table I. Chemical Composition of Pure RPUF Matrix

Materials	Parts by weight (pbw)
Polyether polyol(4110)	100
Catalyst (A-33)	0.5
Catalyst (T12)	0.1
Blowing agent(HCFC-141b)	20.0
Blowing agent (Distilled water)	0.5
Foam stabilizer (Silicone oil)	3.0
Isocyanate(PAPI)	130

In this work, the density of the foams was controlled to about $0.090 \pm 0.005 g/cm^3$.

Characterization

Limiting Oxygen Index (LOI) Test. The LOI test was conducted using an HC-2 oxygen index meter (Jiangning Analysis Instrument Company, China), according to ASTMD2863-97. Dimensions of the samples were $127 \times 10 \times 10$ mm^3.

Cone Calorimeter Test. The cone calorimeter test was performed on a cone calorimeter (Jiangning Analysis Instrument Company, China) according to ISO5660 standard procedures. Square specimens ($100 \times 100 \times 20$ mm^3) were irradiated at a heat flux of 50 KW/m^2.

Thermogravimetric Analysis (TGA). TGA was carried out on a TG 209 F3 (NETZSCH, Germany) thermo-analyzer instrument from 35 to 700°C at a linear heating rate of 10°C/min under a nitrogen atmosphere. The weight of all samples was around 5 mg.

Real-Time Fourier Transform-Infrared Spectra (RT-FT-IR). The RT-FT-IR spectra were recorded using a Nicolet MAGNA-IR750 spectrometer equipped with a heating device having a temperature controller. Powders of the RPUF composites were mixed with KBr powders, and the mixture was pressed into a tablet, which was then placed into the oven. The temperature of the oven was raised at a heating rate of 10°C/min for the dynamic measurement of FT-IR spectra during the thermo-oxidative degradation.

X-ray Photoelectron Spectroscopy (XPS). The XPS Spectra of the char residue (heated in a muffle furnace for 10min at 500°C) were recorded with a Escalab 250 spectrometer (Thermo Scientific Ltd, America), using AI Ka excitation radiation ($hv = 1253.6$eV).

Scanning Electron Microscopy (SEM). SEM was obtained with a JEOL JSM-7500F (JEOL, Japan). The specimens were sputter-coated with a conductive layer.

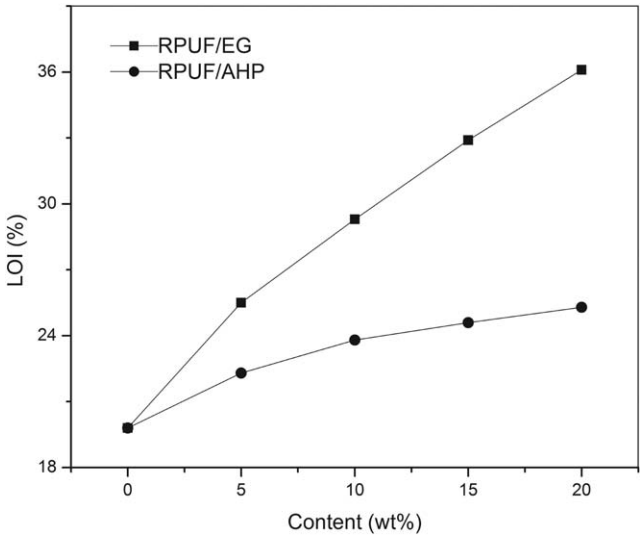

Figure 1. LOI curves of RPUF/EG and RPUF/AHP.

Compression Test. Compression test results were obtained with a 3010 all-purpose electronic test machine (Shenzhen Reger Company, China), according to the standard ASTM D1621-94. The rate of compression was 2 mm min^{-1} at room temperature. The sample size was 50 mm × 50 mm × 50 mm.Five samples were tested to obtain average values.

RESULTS AND DISCUSSION

Flame Retardancy

Figure 1 shows the results of the LOI test of RPUF/EG and RPUF/AHP. The formulations of RPUF composites and the LOI data are shown in Table II. From Figure 1, it can be seen that the LOI value of pure RPUF is only 19.8 vol %, and with the increase of the EG or AHP content, the LOI value of RPUF/EG and RPUF/AHP composites increases. When the EG or AHP content is 20 wt %, the LOI values of RPUF/20EG and RPUF/20AHP are increased to 36.1 vol % and 25.3 vol %, respectively, indicating that the addition of EG or AHP can effectively improve the flame retardant properties of RPUF and the retardancy of EG is better than that of AHP. This may be attributed to the fact that EG can immediately react with sulfuric acid to generate CO_2, SO_2, and H_2O at high temperature to dilute oxygen, which plays an important role in the gas phase flame retardant. Furthermore, these gases make graphite layers expand instantaneously and form a "worm-like" char layer covering the surface of the RPUF foam to not only prevents heat transfer, but limits the diffusion of combustible volatile products towards the flame zone during combustion and oxygen towards the RPUF matrix, preventing the further decomposition of RPUF through the synergistic flame retardant effect between condensed phase and gas phase.[25] However, the main function of AHP takes place in condensed phase.[26] This may be under the influence of heat, and AHP is decomposed to generate aluminum pyrophosphate and aluminum phosphate which can form a stable carbon layer delaying the degradation of RPUF molecular chain. For another reason, the AHP will release PH_3 in the degradation process, and then PH_3 is oxidized into phosphoric acid. Phosphoric acid dehydrates to generate polyphosphoric acid which could promote the degradation of RPUF to form the compacted char layer.[27] The results contribute to the inhibited complete combustion of RPUF molecular chain and protect the RPUF composites.

In order to verify if there is a synergistic effect between the two flame retardants, the total content of the two additives was fixed at 20 wt %, and their ratios were changed. The LOI of RPUF composites are shown in Figure 2. The broken line represents the critical curve. It's obvious that the LOI curve lies above the critical curve, which proves the existence of a synergistic effect between EG and AHP in RPUF composites.[14] The reason for the synergistic effect is that AHP decomposes to generates aluminum pyrophosphate and aluminum phosphate, which are a kind of non-volatile viscous liquid film,[28] increasing the compactness of the char layer derived from the expansion of EG and enhancing the cohesiveness between the char layer and foam matrix to improve the flame retardancy of RPUF. Apart from that, the combined effect of the physical barrier of EG and catalysis of the charring formation of AHP also cause RPUF/EG/AHP composite to have better flame retardant properties.

Table II. Formulations of RPUF Composites and the LOI Data

Sample	RPUF (wt %)	EG (wt %)	AHP (wt %)	LOI (%)
Pure RPUF	100	0	0	19.8
RPUF/5EG	95	5	0	25.5
RPUF/10EG	90	10	0	29.3
RPUF/15EG	85	15	0	32.9
RPUF/20EG	80	20	0	36.1
RPUF/5AHP	95	0	5	22.3
RPUF/10AHP	90	0	10	23.8
RPUF/15AHP	85	0	15	24.6
RPUF/20AHP	80	0	20	25.3
RPUF/15EG/5AHP	80	15	5	37.8
RPUF/10EG/10AHP	80	10	10	36.5
RPUF/5EG/15AHP	80	5	15	32.3

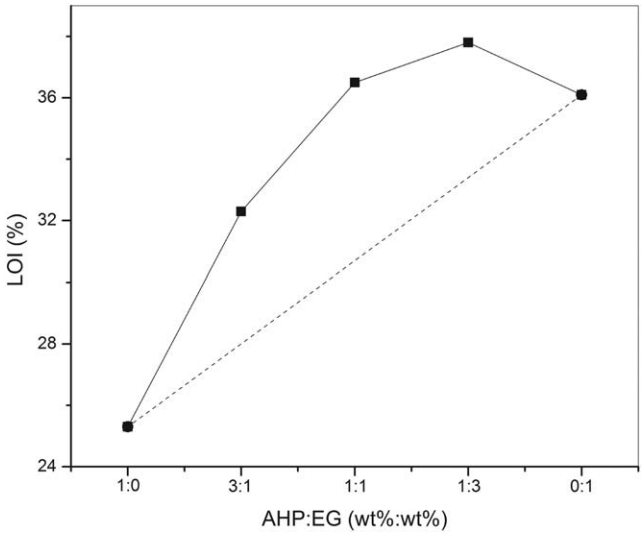

Figure 2. Synergistic effect of EG/AHP systems on the LOI values.

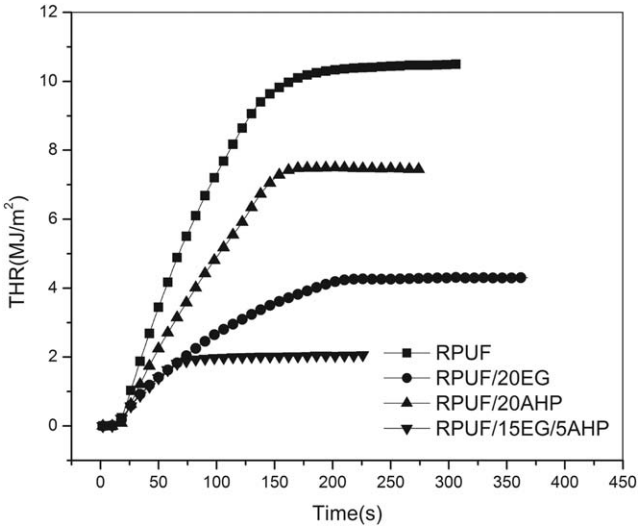

Figure 4. THR curves of pure RPUF and RPUF composites.

Cone Calorimetric Analysis of RPUF Composites

In order to further evaluate the fire safety of the RPUF composites, cone calorimetric analysis was employed. The curves of the heat release rate (HRR) and total heat release (THR) are presented in Figures 3 and 4, and the corresponding data are listed in Table III. It can be seen from Table III that both EG and AHP could reduce the peak heat release rate (pHRR) and HRR values of RPUF composites. With the increasing content of EG or AHP, the pHRR and HRR value is reduced gradually. As shown in Figure 3, the pHRR value is obviously different. The pHRR value of pure RPUF is 108.8 kW/m^2. When 20 wt % EG or AHP is added, the pHRR values of RPUF/20EG and RPUF/20AHP are 55.1 and 76.4 kW/m^2, decreased by 49.4% and 29.8%, respectively, in comparison with pure RPUF. However, when EG is partly replaced by AHP, the pHRR value of RPUF/15EG/5AHP composite is further decreased to 48.8 kW/m^2 on the basis of RPUF/20EG. Meanwhile, it can also be seen from Figure 3 that the HRR value of RPUF/15EG/5AHP composite falls close to 0 sharply in about 75 s, burning ground to a halt. But other samples still keep their heat release and continue to burn. As can been see from Figure 4, all RPUF composites show a lower total heat release than pure RPUF. Furthermore, after the substitution of AHP for part of EG, the THR value of RPUF/15EG/5AHP composite is reduced to 2.1 MJ/m^2 and is much lower than that of RPUF/20EG.

These results prove that EG and AHP create a favorable synergistic effect in flame retardancy, which is consistent with the results of the LOI test. This is because the incorporation of EG and AHP in RPUF composites can form a compact and strong "worm-like" char layer covering in surface of foams to acts as a physical barrier preventing heat and oxygen transfer, thereby reducing the HRR and THR of RPUF composites significantly and improving the flame retardancy of RPUF.

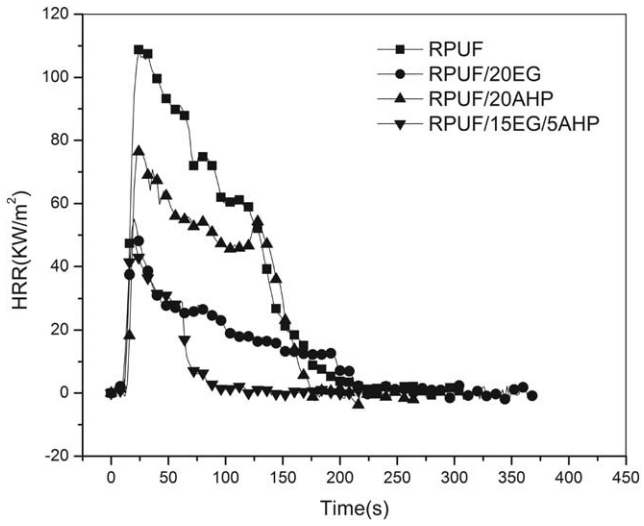

Figure 3. HRR curves of pure RPUF and RPUF composites.

Table III. Cone Calorimeter Data of Pure RPUF and RPUF Composites

Sample	TTI (s)[a]	pHRR (KW/m^2)	THR (MJ/m^2)	Mass loss (wt %)
Pure RPUF	2	108.8	10.5	71.1
RPUF/5EG	2	86.5	8.5	54.9
RPUF/10EG	2	74.9	6.9	42.9
RPUF/15EG	2	65.4	5.1	31.5
RPUF/20EG	2	55.1	4.3	29.1
RPUF/5AHP	2	89.3	9.9	70.2
RPUF/10AHP	2	84.3	7.9	66.6
RPUF/15AHP	3	78.8	7.7	60.4
RPUF/20AHP	3	76.4	7.5	54.2
RPUF/15EG/5AHP	2	48.8	2.1	25.6
RPUF/10EG/10AHP	2	51.0	2.9	28.2
RPUF/5EG/15AHP	3	57.4	7.2	48.4

[a] Time to ignition.

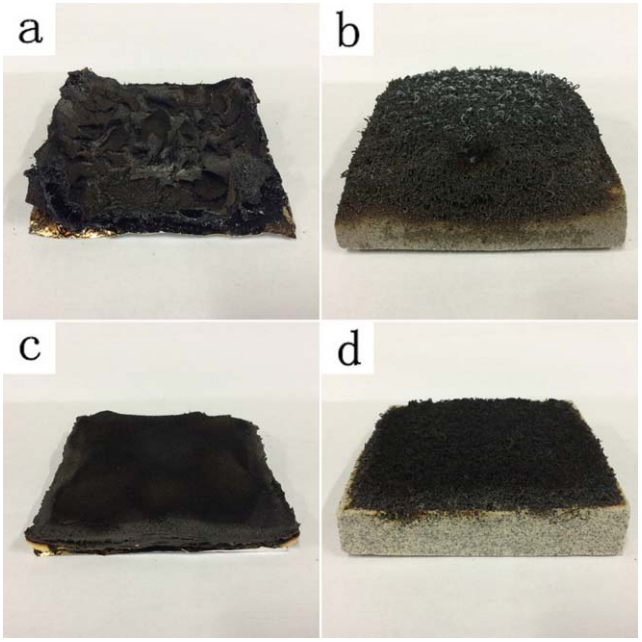

Figure 5. Digital photos of pure RPUF and RPUF composites after cone calorimeter test: (a) pure RPUF; (b) RPUF/20EG; (c) RPUF/20AHP; (d) RPUF/15EG/5AHP. [Color figure can be viewed in the online issue, which is available at wileyonlinelibrary.com.]

Figure 5 presents the digital photos of the residues after the cone calorimeter test. As can be observed, there is rarely residue for pure RPUF after burning and the char layer is broken. Figure 5(b) shows the residue of RPUF/20EG, which exhibits a significant intumescent but incompact char layer. The residue of RPUF/20AHP [Figure 5(c)] displays a compact char layer. However, the residue of RPUF/15EG/5AHP, as shown in Figure 5(d), shows a compact, intumescent and strong char layer, suggesting the combination of AHP and EG could provide better flame retardancy for RPUF/AHP/EG composite.

Thermal Properties

The TGA and DTG curves of pure RPUF and RPUF composites under nitrogen atmosphere are shown in Figures 6 and 7, and the corresponding data are listed in Table IV. Pure RPUF shows the onset degradation temperature ($T_{-5\%}$) and T_{max} at 266.2°C and 339.7°C, respectively. The $T_{-5\%}$ of RPUF/20EG composites is lower than that of pure RPUF while RPUF/20AHP composites exhibit a higher onset decomposition temperature. It may be connected with the decomposition temperature of EG and AHP, where the decomposition temperature of EG is lower while that of AHP is higher. All RPUF composites exhibit lower T_{max} than that of pure RPUF, no matter whether EG and AHP are used alone or together. It is interesting to find that the T_{max} of RPUF/15EG/5AHP composites is higher than that of RPUF/20EG and RPUF/20AHP, indicating that the addition of both EG and AHP increases the thermal stability of RPUF composites.

From Figure 6, the char residue of pure RPUF is 18.7% at 700°C, but RPUF/20EG and RPUF/20AHP present the char residue of 35.0 wt % and 32.2 wt %, respectively, indicating that the addition of EG or AHP increases the thermal stability of RPUF composites at high temperature. Furthermore, it can been see from Figure 6, when EG is partly replaced by AHP, the char residue of RPUF/15EG/5AHP is 35.9 wt % higher than that of composites filled with EG or AHP separately, which indicates that the addition of AHP can promote the formation of a system char layer, further confirming that there is a synergistic effect between EG and AHP at the enhanced high-temperature stability of RPUF composites.

RT-FT-IR Analysis of RPUF Composites

In order to study the process of thermal degradation of the composites, a RT-FT-IR analysis was employed. The FT-IR spectra of pure RPUF, RPUF/20EG, RPUF/20AHP, and RPUF/15EG/5AHP are presented in Figure 8. As can be seen from Figure 8, the FT-IR spectra of all samples show a similar absorption peak at room temperature. The absorption peaks near 3380 cm^{-1} and 1520 cm^{-1} can be assigned to the stretching vibration and

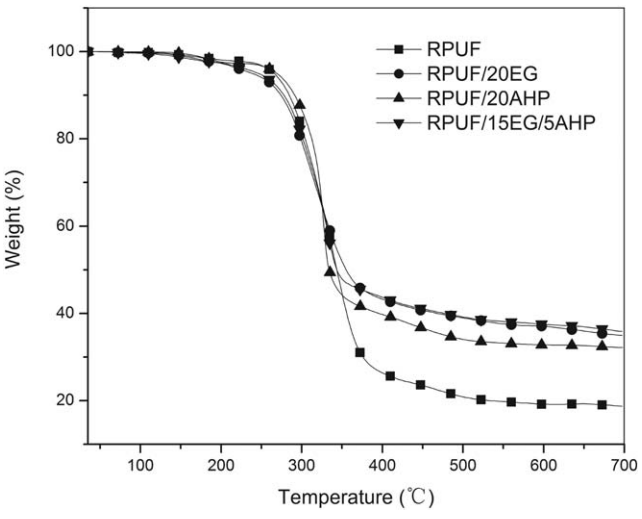

Figure 6. TGA curves of pure RPUF and RPUF composites.

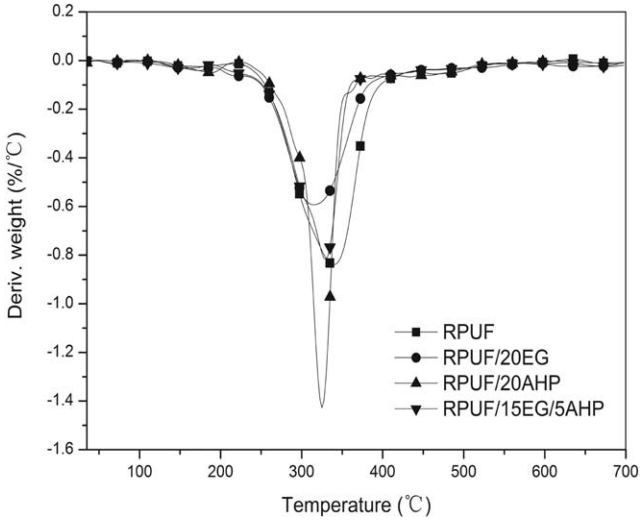

Figure 7. DTG curves of pure RPUF and RPUF composites.

Table IV. TGA and DTG Data of Pure RPUF and RPUF Composites

Sample	$T_{-5\%}$ (°C)[a]	$T_{-50\%}$ (°C)[b]	T_{max} (°C)[c]	Char residue at 700°C (%)
RPUF	266.2	343.5	339.7	18.7
RPUF/20EG	239.6	355.1	315.2	35.0
RPUF/20AHP	269.0	334.2	325.0	32.2
RPUF/15EG/5AHP	246.3	343.7	329.8	35.9

[a] The temperature at 5 wt % mass loss.
[b] The temperature at 50 wt % mass loss.
[c] The temperature at the maximum weight loss.

the in-plane bending vibration of N-H. The 2925 cm^{-1} and 2870 cm^{-1} absorption peaks are caused by the stretching vibration of C-H in methyl and methylene. The peaks around 1725 cm^{-1} and 1213cm^{-1} are typical for the stretching vibration of esters C═O and C—O, respectively. And the peak near 1090 cm^{-1} belongs to the C—O—C stretching vibration. With the increase of temperature, the changes of FT-IR spectra for four samples are similar, and the weakened intensity of these bands is caused by the gradual degradation of the molecular chain of RPUF matrix. But when the temperature rise to 330°C, the FT-IR spectra of four samples begin to dispaly obvious differences and are mainly divided into two aspects: firstly, there are absolutely no absorption peaks near 1260 to 1085 cm^{-1} in the FT-IR spectra of pure RPUF and RPUF/20EG. In contrast,

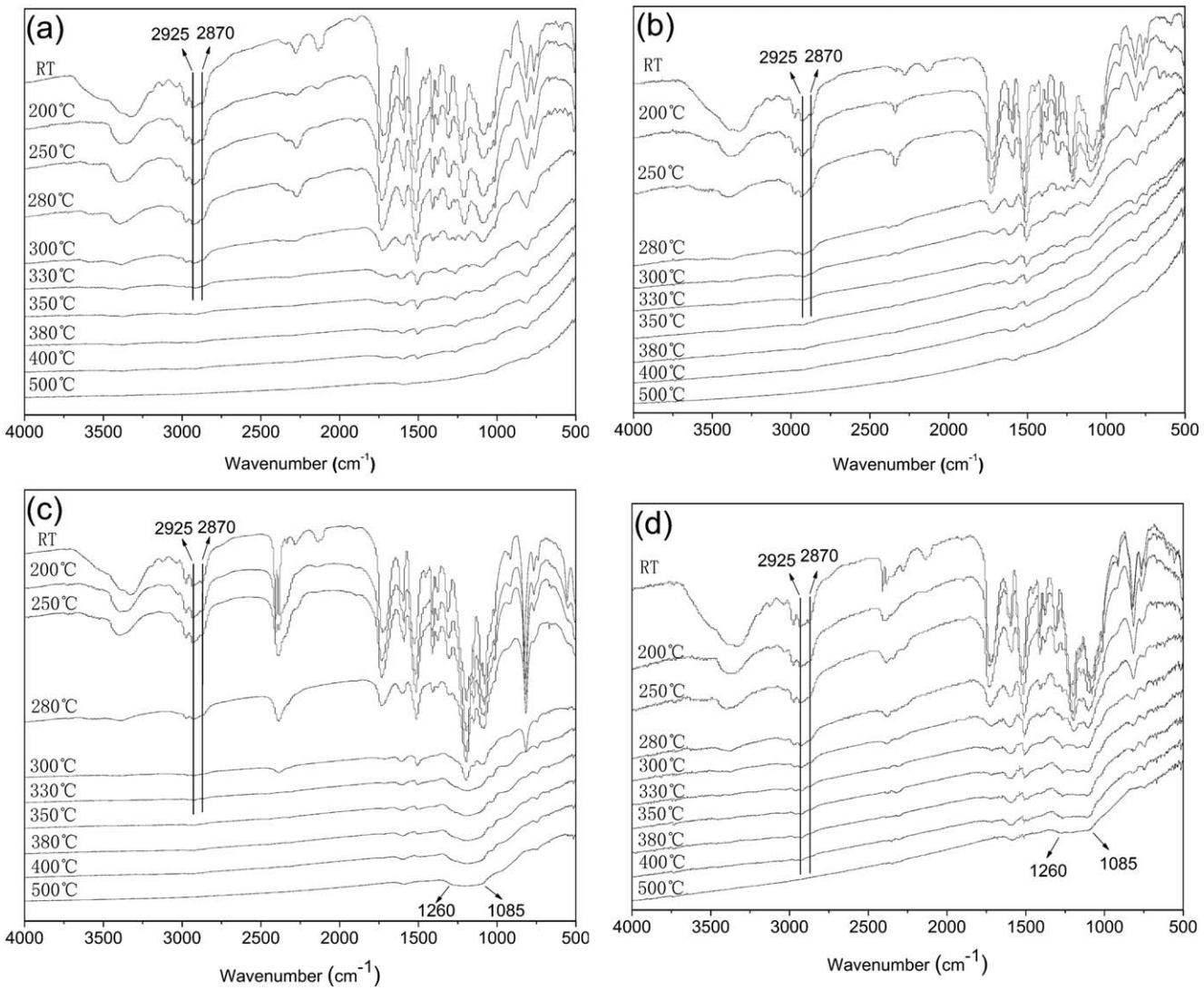

Figure 8. RT-FT-IR spectra of RPUF composites at different pyrolysis temperatures: (a) pure RPUF, (b) RPUF/20EG, (c) RPUF/20AHP, (d) RPUF/15EG/5AHP.

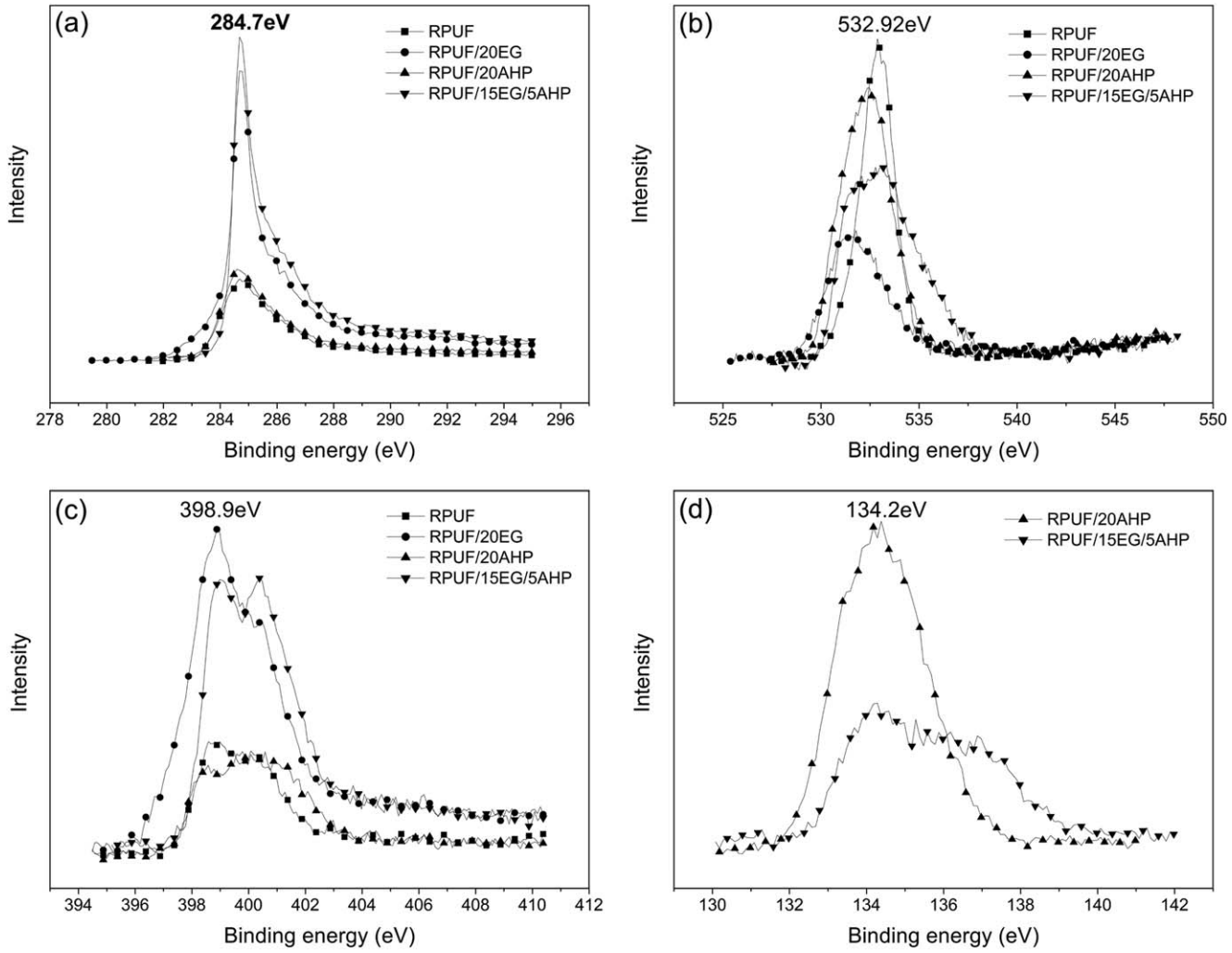

Figure 9. (a) C_{1S}, (b) N_{1S}, (c) O_{1S}, and (d) P_{2P} XPS spectra of char residue of RPUF composites.

these peaks still exist in the spectra of RPUF/20AHP and RPUF/15EG/5AHP, which is caused by the addition of AHP in the samples. At room temperature, the absorption peaks of phosphorus-oxide in AHP overlap with the bands of C—O and C—O—C in polyurethane leading to the difference is not obvious for four spectra of Figure 8. After the decomposition of C—O and C—O—C with the increasing temperature, the absorption peaks of phosphorus-oxide in AHP are revealed. The peak at 1260 cm^{-1} is assigned to the stretching vibration of P═O, and the peak at 1085 cm^{-1} is attributed to the P—O—P.[29] In Figure 8(c,d), the apparent wide peak at 1260 to 1085 cm^{-1} that contributes to the polyphosphoric acid formed during the degradation process of RPUF composites containing AHP can promote the formation of the compact char layer. Secondly, the peaks around 2900 cm^{-1} almost disappear at 330°C for the pure RPUF, RPUF/20EG, and RPUF/20AHP compared with Figure 8(a–d). However, these peaks still exist at 400°C and almost disappear at 500°C for RPUF/15EG/5AHP. Usually, the absorption peaks of aliphatic C—H bond in the range of 2800 to 3000 cm^{-1} are used to evaluate the thermal oxidation stability of polymer.[30,31] This is because with the increase of temperature, the polymer molecular chain degrades gradually, causing the intensity of the absorption peaks of C—H bond to weaken gradually and the absorption peaks of C—H bond almost

Table V. XPS Results of the Char Residue of RPUF Composites

Sample	C (at. %)	O (at. %)	N (at. %)	P (at. %)	Al (at. %)	N/C
Pure RPUF	58.27	30.36	11.37	-	-	0.195
RPUF/20EG	74.93	9.65	15.42	-	-	0.206
RPUF/20AHP	48.52	29.34	10.43	7.77	3.95	0.215
RPUF/15EG/5AHP	67.59	16.03	12.01	2.7	1.67	0.237

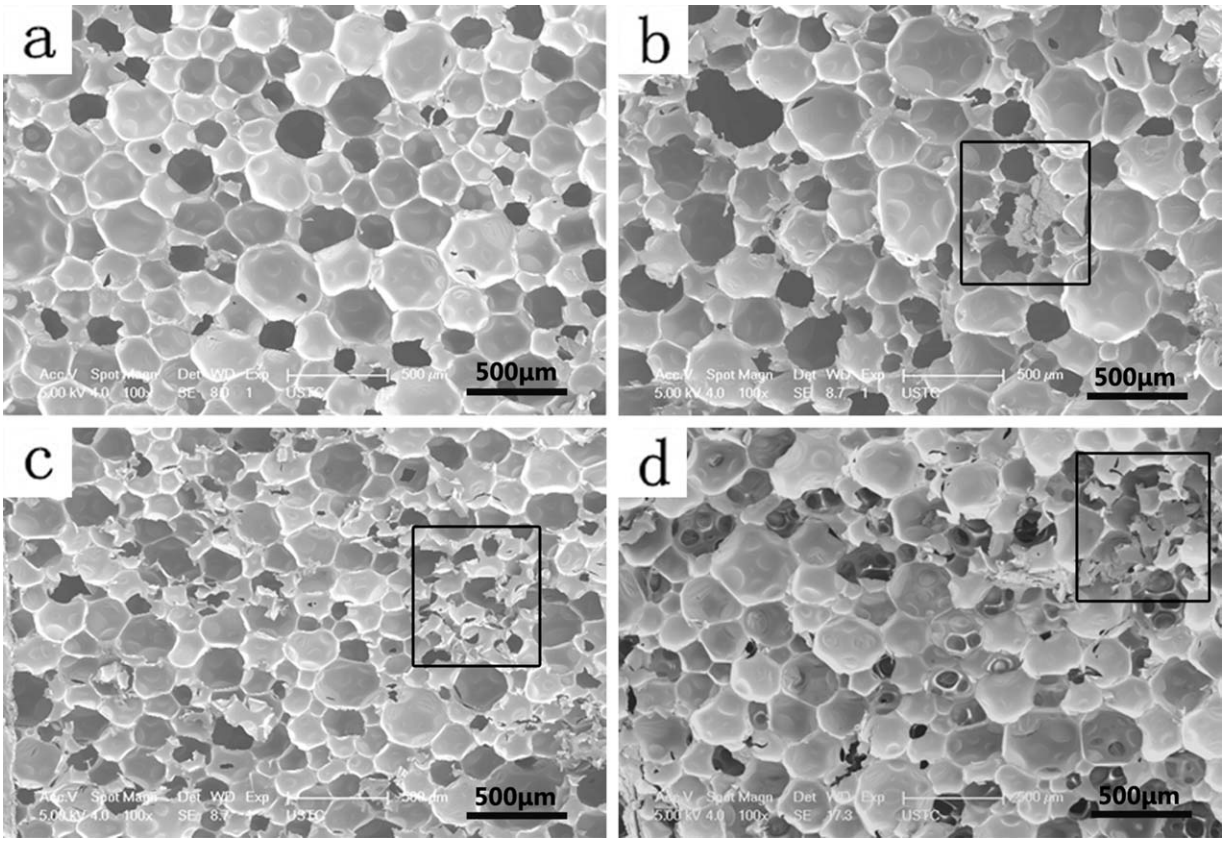

Figure 10. SEM images of pure RPUF and RPUF composites: (a) pure RPUF; (b) RPUF/20EG; (c) RPUF/20AHP; (d) RPUF/15EG/5AHP.

disappear when the polymer molecular chain degrades completely. The higher the corresponding temperature of disappearing peak implies the higher thermal stability of the material. The higher heat resistance of RPUF/15EG/5AHP composite indicates that there is a synergistic effect between EG and AHP.

XPS Analysis of Residual Char of RPUF Composites

Figure 9 shows the XPS spectra of pure RPUF, RPUF/20EG, RPUF/20AHP, and RPUF/15EG/5AHP. The data of the XPS are presented in Table V. The peak at 284.7 eV is attributed to C—C and C—H in aliphatic and aromatic.[32] The peak at 532.9 eV is assigned to —O— in C—O—C, C—O—P, and/or P—O—P groups, and the peak at 134.2 eV can be attributed to the phosphorus in the pyrophosphate and polyphosphate structure.[33] For the N_{1s} spectrum, the peak at 398.9 eV can be assigned to C—N or C═N.[34] Usually, urethane groups in the molecular chain firstly depolymerize to alcohols and isocyanate in the polyurethane thermal decomposition process, and relatively stable compounds containing C—N and C═N are generated during the dimerization and trimerization reaction between isocyanate.[35,36] In the combustion process, the N elements in polyurethane molecular chain not only volatilize with the formation of gas such as HCN, NO_2, but form relatively stable compounds containing C—N and C═N in the char residues. The higher relative content of N element in the char residue, the more stable compounds containing N element, and the higher thermal stability the material has.

Before burning, compared with pure RPUF and RPUF/20EG, the N/C ratio of the RPUF/20EG system is lower in theory, but the N/C ratio of RPUF/20EG residue char is greater than that of pure RPUF after burning. For pure RPUF and RPUF/20AHP samples, the N/C ratio is supposed to be the same, but the N/C ratio of RPUF/20AHP residue char is also greater than that of pure RPUF after burning. The improvement of the N/C ratio

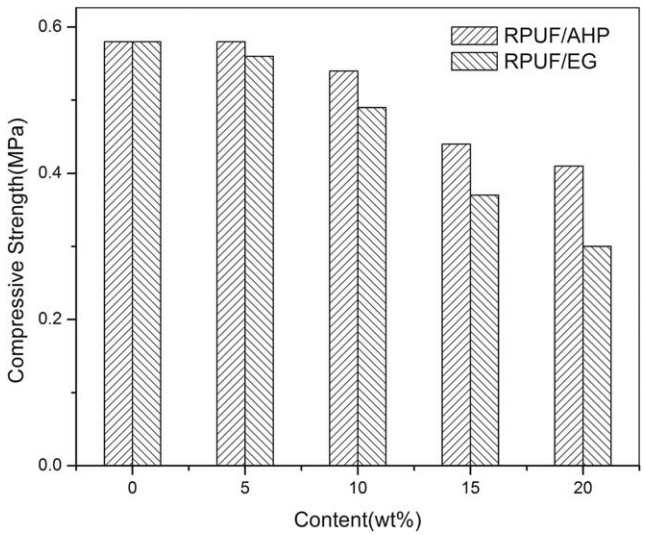

Figure 11. Compressive strength of EG, AHP-filled RPUF with various contents.

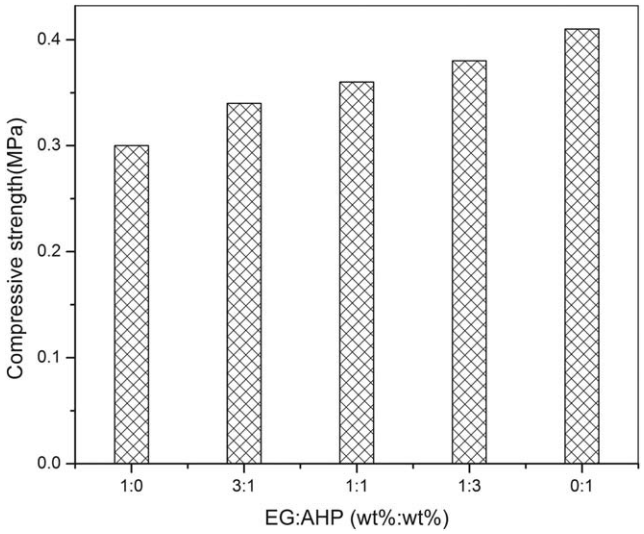

Figure 12. Compressive strength of EG, AHP-filled RPUF with various EG/AHP ratios.

indicates that the relative content of N element in residue char is improved, which shows that both EG and AHP can improve the flame retardant properties of composite materials. For RPUF/15EG/5AHP, the N/C ratio is between RPUF/20EG and RPUF/20AHP before burning. But after combustion, the N/C ratio of the residue char of RPUF/15EG/5AHP is at maximum, suggesting that the combination of EG and AHP enables composites to have a better flame retardancy. In addition, the XPS spectra analysis of char residue indicates that RPUF samples with AHP added generate a char layer with abundant phosphorus elements after thermal degradation, which suggests that AHP mainly play a role in the condensed phase and participates in the formation of a char layer in the thermal degradation process, thus delaying the further degradation of the material.

Morphology of RPUF Composites

Figure 10 shows the SEM micrographs of pure RPUF, EG, and AHP-filled RPUF. For pure RPUF shown in Figure 10(a), the cell shape is closed cellular polyhedron with no collapse or collision in the cell system. In addition, not only are the diameters of the cells approximately uniform but the cell walls are integrated. Figure 10(b–d) presents SEM micrographs of RPUF/20EG, RPUF/20AHP, and RPUF/15EG/5AHP composites, respectively. From Figure 10(b–d), we can see that the appearance of EG, AHP or EG/AHP destroys the integrity of the cell structure in different degrees (marked with rectangle) compared with pure RPUF. This is because the addition of solid filler EG or AHP causes the increased viscosity of the mixture, making it more difficult to disperse uniformly and leading to the aggregation of EG and AHP at the RPUF matrix. What is more, the larger EG flakes and AHP particles also damage cell structure.

Figure 10(d) shows the micrograph of the RPUF filled with EG and AHP at a weight ratio of 3 : 1. Compared with the micrograph of RPUF/20EG, we can discover that the cells structure of RPUF/15EG/5AHP composites is less destroyed. This indicates that partial substitution of EG with AHP can reduce the effects of EG on the frame of the RPUF composite. This is due to the fact that the small-sized AHP particles cause less damage to the bubble hole structure of RPUF composite compared with the EG flakes, keeping the cell structure of RPUF/15EG/5AHP composites intact.

Compressive Strength

To verify the function of EG or AHP-filled RPUF, the compressive strength of the composites with different contents in the matrix was measured. Figure 11 presents the variations of the compressive strength with various EG or AHP contents. From Figure 11, it can be seen that the compressive strength is reduced with the addition of EG or AHP into the RPUF matrix. With the increasing content of these additions, the compressive strength is decreased. This is because EG and AHP are inorganic materials and the incompatibility of these additives with the RPUF matrix damages the RPUF matrix to a certain extent, leading to a decrease of compressive strength.

Figure 12 presents the variations of the compressive strength with various EG/AHP ratios, and the total addition of EG or AHP is 20 wt %. Figure 12 demonstrates that with the increase of the AHP content, the compressive strength of RPUF/EG/AHP composites is increased. For instance, when the loading of flame retardant is 20 wt %, the compressive strength of RPUF/15EG/5AHP is higher than that of RPUF/20EG.It can be inferred that partial substitution of EG with AHP could decrease the effects of the EG flakes on the mechanical properties of RPUF composites. It's also due to the fact that the appearance of EG damages the RPUF matrix cells obviously, but the size of AHP is smaller than that of EG, so AHP has less damage to the RPUF matrix cells, and as a result, the integrality of RPUF is well preserved.

CONCLUSION

Both EG and AHP could improve the flame retardency of RPUF composites efficiently. When the flame-retardant loading is 20 wt %, the LOI value of RPUF/20AHP is increased to 25.3 vol %, while the LOI value of RPUF/20EG can reach 36.1 vol %, which indicates that EG can improve the flame-retardant property of RPUF more effectively than AHP. Moreover, when the total addition of EG and AHP is 20 wt %, the weight ratio of EG and AHP is 3 : 1, the LOI value of RPUF/15EG/5AHP composites reaches the highest at 37.8 vol %. In addition, cone calorimeter test results of all filled RPUF samples show lower HRR and THR than pure RPUF. And when EG is partly replaced by AHP, the HRR and THR of RPUF/15EG/5AHP is the lowest. TGA results show that, with a partial substitution of EG with AHP, the thermal stability of composites is higher than those with components used singly. The combination of EG and AHP could improve the char residue which provides better flame retardancy for RPUF composites. The thermal degradation process of RPUF composites and the chemical components of the char residue were investigated by RT-FT-IR and XPS, respectively. And the results prove that RPUF/15EG/5AHP has higher heat resistance in the later stage.

All investigation results also prove that the existence of a synergistic effect with EG and AHP in RPUF composites. This is because the incorporation of EG and AHP in RPUF composites

could form a compact and strong "worm-like" char layer covering the surface of foams to act as a physical barrier preventing heat and mass transfer, leading to a delayed complete combustion of the material.

Although EG and AHP show an outstanding flame retardant property, they destroy the cell structure to a certain extent, and display lower compressive strength than pure RPUF. However, compared with the RPUF composites only filled with EG, a better cell structure and mechanical property are chieved with partial substitution of EG with AHP.

ACKNOWLEDGMENTS

The authors are grateful to the Research Fund for the Doctoral Program of Anhui Jianzhu University (2014) and National Key Technology R&D Program (2013BAJ01B05) for their financial support.

REFERENCES

1. Zhang, L. Q.; Zhang, M.; Zhou, Y. H.; Hu, L. H. *Polym. Degrad. Stab.* **2013**, *98*, 2784.
2. Bian, X. C.; Tang, J. H.; Li, Z. M. *J. Appl. Polym. Sci.* **2008**, *109*, 1935.
3. Qian, L. J.; Feng, F. F.; Tang, S. *Polymer* **2014**, *55*, 95.
4. Usta, N. *J. Appl. Polym. Sci.* **2012**, *124*, 3372.
5. Cheng, J. J.; Shi, B. B.; Zhou, F. B.; Chen, X. Y. *J. Appl. Polym. Sci.* **2014**, *131*, 40253.
6. Gao, L. P.; Zheng, G. Y.; Zhou, Y. H.; Hu, L. H.; Feng, G. D.; Zhang, M. *Polym. Degrad. Stab.* **2014**, *101*, 92.
7. Tan, S. Q.; Abraham, T.; Ference, D.; Macosko, C. W. *Polymer* **2011**, *52*, 2840.
8. Zhang, X. G.; Ge, L. L.; Zhang, W. Q.; Tang, J. H.; Ye, L.; Li, Z. M. *J. Appl. Polym. Sci.* **2011**, *122*, 932.
9. Wang, W. J.; He, K.; Dong, Q. X.; Zhu, N.; Fan, Y.; Wang, F.; Xia, Y. B.; Li, H. F.; Wang, J.; Yuan, Z.; Wang, E.; Lai, Z. F.; Kong, T.; Wang, X.; Ma, H. W.; Yang, M. S. *J. Appl. Polym. Sci.* **2014**, *131*, 39936.
10. Ye, L.; Meng, X. Y.; Liu, X. M.; Tang, J. H.; Li, Z. M. *J. Appl. Polym. Sci.* **2009**, *111*, 2372.
11. Zhang, A. Z.; Zhang, Y. H.; Lv, F. Z.; Chu, P. K. *J. Appl. Polym. Sci.* **2013**, *128*, 347.
12. Zhang, M.; Zhang, J. W.; Chen, S. G.; Zhou, Y. H. *Polym. Degrad. Stab.* **2014**, *110*, 27.
13. Thirumal, M.; Khastgir, D.; Nando, G. B.; Naik, Y. P.; Singha, N. K. *Polym. Degrad. Stab.* **2010**, *95*, 1138.
14. Wang, C. Q.; Ge, F. Y.; Sun, J.; Cai, Z. S. *J Appl. Polym. Sci.* **2013**, *130*, 916.
15. Shi, L.; Li, Z. M.; Xie, B. H.; Wang, J. H.; Tian, C. R.; Yang, M. B. *Polym. Int.* **2006**, *55*, 862.
16. Meng, X. Y.; Ye, L.; Zhang, X. G.; Tang, P. M.; Tang, J. H.; Ji, X.; Li, Z. M. *J. Appl. Polym. Sci.* **2009**, *114*, 853.
17. Thirumal, M.; Khastgir, D.; Singha, N. K.; Manjunath, B. S.; Naik, Y. P. *J. Appl. Polym. Sci.* **2008**, *110*, 2586.
18. Li, H. X.; Ning, N. Y.; Zhang, L. Q.; Wang, Y. X.; Liang, W. L.; Tian, M. *Polym. Degrad. Stab.* **2014**, *105*, 86.
19. Wu, N. J.; Li, X. T. *Polym. Degrad. Stab.* **2014**, *105*, 265.
20. Yang, W.; Song, L.; Hu, Y.; Lu, H. D.; Yuan, R. K. *Compos. B* **2011**, *42*, 1057.
21. Yan, Y. W.; Huang, J. Q.; Guan, Y. H.; Shang, K.; Jian, R. K.; Wang, Y. Z. *Polym. Degrad. Stab.* **2014**, *99*, 35.
22. Yuan, B. H.; Bao, C. L.; Guo, Y. Q.; Song, L.; Liew, K. M.; Hu, Y. *Ind. Eng. Chem. Res.* **2012**, *51*, 14065.
23. Lorenzetti, A.; Modesti, M.; Gallo, E.; Schartel, B.; Besco, S.; Roso, M. *Polym. Degrad. Stab.* **2012**, *97*, 2364.
24. Yang, H. Y.; Wang, X.; Song, L.; Yu, B.; Yuan, Y.; Hu, Y.; Yuan, R. K. K. *Polym. Adv. Technol.* **2014**, *25*, 1034.
25. Duan, H. J.; Kang, H. Q.; Zhang, W. Q.; Ji, X.; Li, Z. M.; Tang, J. H. *Polym. Int.* **2014**, *63*, 72.
26. Sullaltia, S.; Colonnaa, M.; Berti, C.; Fiorini, M.; Karanam, S. *Polym. Degrad. Stab.* **2012**, *97*, 566.
27. Tang, G.; Wang, X.; Xing, W. Y.; Zhang, P.; Wang, B. B.; Hong, N. N.; Yang, W.; Hu, Y.; Song, L. *Ind. Eng. Chem. Res.* **2012**, *51*, 12009.
28. Qu, H. Q.; Liu, X.; Xu, J. Z.; Ma, H. Y.; Jiao, Y. H.; Xie, J. *Ind. Eng. Chem. Res.* **2014**, *53*, 8476.
29. Hu, S.; Song, L.; Pang, H. F.; Hu, Y.; Gong, X. L. *J. Anal. Appl. Pyrolysis* **2012**, *97*, 109.
30. Xie, R. C.; Qu, B. J.; Hu, K. L. *Polym. Degrad. Stab.* **2001**, *72*, 313.
31. Lin, J. S.; Liu, Y.; Wang, D. Y.; Qin, Q.; Wang, Y. Z. *Ind. Eng. Chem. Res.* **2011**, *50*, 9998.
32. Wang, X.; Xuan, S. Y.; Song, L.; Yang, H. Y.; Lu, H. D.; Hu, Y. *J. Macromol. Sci. Phys.* **2012**, *51*, 255.
33. Shan, X. Y.; Song, L.; Xing, W. Y.; Hu, Y.; Lo, S. M. *Ind. Eng. Chem. Res.* **2012**, *51*, 13037.
34. Chen, X. L.; Hu, Y.; Jiao, C. M.; Song, L. *Polym. Degrad. Stab.* **2007**, *92*, 1141.
35. Velencoso, M. M.; Ramos, M. J.; Klein, R.; Lucas, A. D.; Rodriguuz, J. F. *Polym. Degrad. Stab.* **2014**, *101*, 40.
36. Berta, M.; Lindsay, C.; Pans, G.; Camino, G. *Polym. Degrad. Stab.* **2006**, *91*, 1179.